Perspective

Approaches to quantify axonal morphology for the analysis of axonal degeneration

Alex Palumbo, Marietta Zille[*]

Morphological hallmarks of axonal degeneration (AxD): Axons transmit signals from one neuron to another and are crucial for the proper communication in the nervous system. Therefore, the disintegration of axons, a process named AxD, has detrimental consequences and plays a key role in many neurological diseases.

AxD is characterized by the formation of two morphological hallmarks, namely axonal fragments and axonal swellings. Whereas axonal fragments are separated segments of the axon resulting from axonal breakdown, axonal swellings are spherical structures that may emerge along the axon prior to the formation of axonal fragments (Palumbo et al., 2021). Quantifying these morphological hallmarks enables researchers to follow AxD over time, better understand differences in AxD kinetics, and assess candidate treatments.

Here, we give a brief overview of the different approaches to quantify AxD based on axonal morphology and explain how recent machine learning tools may be used to decipher the progression of AxD to further our understanding of this process and develop novel therapeutic interventions.

Image binarization and manual labeling to quantify AxD: A widely applied approach to analyze AxD is the AxD index (or relative neurite/axonal integrity), the ratio of the fragmented axon area over the total axon area (Sasaki et al., 2009; Arrázola et al., 2019). To identify axons and axonal fragments, grey-scale microscopic images are converted to binary images by thresholding. Pixels are thereby assigned to background, axons or axonal fragments. Structures that are continuously connected are counted as axons, whereas axonal fragments are identified as non-connected structures and counted using the particle analyzer module of ImageJ. Further measures of AxD are: i) the distance between lesion site and axonal tip, ii) the distance between fragments, iii) the length of the axonal fragments, and iv) fragmentation rate. The above-described approaches can be applied in vitro, ex vivo, and also in vivo (Kerschensteiner et al., 2005; Knöferle et al., 2010; Gerdts et al., 2015; Canty et al., 2020). For the latter, fluorescently labeled axonal tracts using transgenic mice or viruses are required. However, image binarization is not always sensitive enough to recognize thin axons, which are then either omitted or misinterpreted as axonal fragments. Another drawback of image binarization is that it cannot be used to quantify axonal swellings.

Approaches to investigate the occurrence of axonal swellings in in vitro, ex vivo, and in vivo experiments involve calculating i) the ratio of the number of axonal swellings compared to the axon length by manual labeling of regions of interest using ImageJ (Yong et al., 2019) and ii) the axonal swelling density measuring pixel intensity per axon length using MATLAB (Canty et al., 2020). As is the case for image binarization, these approaches are semi-automatic and subjective, because they require manual annotation, and thus are very time-consuming. Hence, a tool to analyze axonal morphology including both hallmarks of AxD — axonal swellings and axonal fragments — that is more objective and can be used automatically would be of great use to the scientific community.

Principle of deep learning to classify structures in microscopic images: Recent progress in the field of machine learning has opened novel ways of how to quantify axonal morphology on microscopic images. Convolutional neural networks (CNNs) represent a deep learning approach to classify specific structures in microscopic images (Yang and Wang, 2020; **Figure 1**). A CNN consists of three different layers, namely input, hidden, and output layer, containing several nodes whose connection strengths are defined by weights.

In the input layer, the CNN receives information about the dimensions of the images as input pixel values. The backbone of a CNN is the extraction of pixel information in the hidden layer by convolutional operations to recognize edges, lines, specific shapes, and gradient orientation. Convolutional operations are based on the application of different filters, also named kernels, that slide as a small window region over the image and calculate the sum of pixel values.

To minimize the computational power necessary to process the data by reducing the image size, further pooling operations are employed for each area of the image covered by the kernel. During pooling, either the maximum or the average pixel value of the kernel covering an area of the image is extracted. Each pixel value originating from different kernels is then multiplied by an associated weight and transformed by a mathematical activation and normalization function to activate the node as it incorporates several weighted inputs. The activated node then propagates the information to several subsequent nodes in the next layer which differently weigh the input. These weight-associated node activations eventually determine which nodes are most strongly connected.

In the output layer, the probabilities of classifying specific structures in the microscopic image are calculated leading to the assignment of each pixel to a class (semantic image segmentation) as output. The resulting segmented image containing the classified pixels is then compared to the original image. A mathematical operation called "backpropagation" is eventually used to re-adjust the weights among the nodes in each layer to ensure that the output prediction of the CNN corresponds to the original image.

This learning process can be performed by the CNN itself or be taught via supervised learning (Yang and Wang, 2020). In the case of supervised learning, several microscopic images are annotated by experts. The original microscopic images and their annotations are "fed" into the CNN and used for output comparisons. Finally, the performance of a CNN to match the original image should be validated using independent datasets and compared against expert raters.

Deep learning-based approaches to quantify AxD: Several CNNs have recently been developed for the recognition of axonal morphologies (**Box 1**). TrailMap facilitates the 3D visualization of axonal projections in cleared brain tissue (Friedmann et al., 2020). The authors adapted the AdipoClear protocol to reduce the autofluorescence of myelin and axons of healthy brains that were fluorescently labeled by viral-genetic strategies. The recognized axons were then aligned to the different brain regions using the Allen Brain Atlas Common Coordinate Framework as a standard reference space. Using this approach, the authors were able to quantify axonal density within noisy whole-brain volumetric data. However, this tool is not suitable to determine AxD as it has not been trained to distinguish between healthy axons and axons undergoing AxD. In addition, although TrailMap identifies differently labeled axons originating from various neuron types, the resulting visualization does not discriminate between axons and dendrites.

Another tool developed by Schubert et al. (2019) allows to distinguish between neuronal substructures (axons, dendrites, and somata) using cellular morphology neural networks (CMN) based on multi-view projections. These networks combine unsupervised and supervised learning approaches to analyze electron microscopy images. In addition to the reconstruction of different neuronal substructures, the authors were also able to distinguish between various neuron types and glial cells. Despite the advantage of cellular morphology neural networks to reconstruct the axonal 3D shape from several multi-view 2D images, they have not been specifically developed to reconstruct fragmented axons.

AxonDeepSeg is another supervised CNN that can be used to segment axons and myelin in cross-sectional electron microscopy images of brain and spinal cord tissue (Zaimi et al., 2018). The authors provide two ready-to-use models for scanning and transmission electron microscopy and demonstrated high segmentation accuracy across different species and tissues. Although this method allows to calculate the volume, diameter, and density of axons and myelin, which can be used as estimates to evaluate AxD, it does not consider axonal swellings as a direct morphological hallmark of AxD.

For axonal swelling recognition, Cheng et al. (2019) developed the DeepBouton supervised CNN. It counts the overall number of axonal swellings along individual neurons based on the different sizes and fluorescence intensities in confocal images of the whole brain of mice that the authors acquired by high-resolution stage-scanning microscopy. The method is superior to other conventional methods and can be used to detect axonal swellings in different neuron types.

Whereas whole brain or tissue section imaging is useful to determine AxD ex vivo at specific time points, it does not allow to examine the progression of AxD over time and to study the molecular machinery underlying AxD in its detail.

Cell culture systems allow to study spatially isolated axons by using a media volume difference that generates a microflux between a soma compartment and an axonal compartment. This microflux drives the outgrowth of axons from the soma compartment into the axonal compartment. Axons and somata can then be separately manipulated to assess different AxD stimuli. Recently, we have developed a microflux-based cell culture system and the CNN-based deep learning tool EntireAxon to quantify axons, axonal fragments, and axonal swellings on microscopic phase-contrast images for AxD assessment (Palumbo et al., 2021). This allows the continuous detection of AxD over time without the need of expressing fluorescently labeled proteins or the fixation of the axons at different time points. The EntireAxon is trained to recognize the occurrence of axons, axonal swellings, and axonal fragments by segmenting each pixel of the image that is then classified as background, axon, axonal swelling, or axonal fragment. Further application of the EntireAxon on fluorescent images is also possible (Menon et al., 2020).

Based on the acquired data on the changes of morphological hallmarks of AxD over time, we were able to detect four morphological patterns of AxD (granular, retraction, swelling, and transport degeneration) in a model of AxD in hemorrhagic stroke (Palumbo et al., 2021). The EntireAxon tool cannot only assess AxD by quantifying the morphological hallmarks of AxD, but also determine the morphological heterogeneity of degenerating axons. This versatility may allow to expand our understanding of AxD in the context of neurological diseases. However, the EntireAxon CNN cannot be used to determine AxD on 3D images. Features such as branching, lengths, and diameters as well as tracking of axonal cargo transports are also of high relevance and subject of future development.

One of the main limitations of the currently available deep learning-based approaches is that they cannot quantify AxD in vivo. In the future, it is thus important to generate and share datasets to train CNNs that include in vivo microscopic recordings of axons undergoing AxD over time, which will enable the analysis of AxD progression in animal models. In addition, one of the general limitations in training neural networks is the availability of training data, which must be annotated manually by experts. To reduce labeling costs, active learning approaches can be applied to identify the images that yield the best results (Grüning et al., 2020), thereby saving time to implement or modify existing deep learning-based approaches.

Conclusions: Recent deep learning-based approaches have significantly improved our abilities to quantify axonal morphological changes ensuring objectivity and automatization in the analysis process without the need for manual annotation and thresholding. This is of high importance to allow systematic investigation and to increase our understanding of the mechanisms underlying AxD. Together with enhanced throughput test systems, this will form a platform for the assessment of new drug candidates to prevent and treat AxD in many neurological diseases.
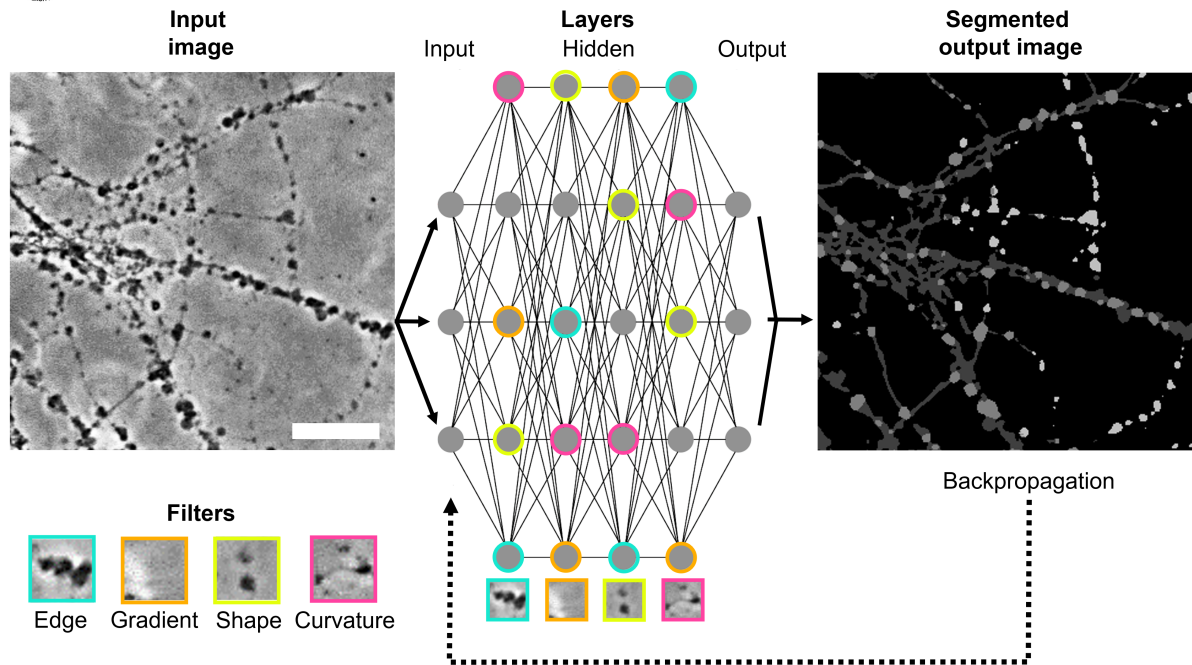
Figure 1 | Schematic illustration of the recognition of the morphology features of AxD by a CNN.
A microscopic image containing axonal features (axons, axonal swellings, and axonal fragments) is introduced to the CNN as an input image. Each node of the input layer forwards dimensional pixel values to the hidden layers for structural information extraction via convolutional and pooling operations. In each of the hidden layers, nodes employ different filters (e.g., cyan filter for edges, orange filter for gradients, yellow filter for shapes, and purple filter for curvatures) and propagate the information to the nodes of the subsequent layer until reaching the output layer. In the output layer, all information is integrated to fully segment the input image. To correct potential errors in the output prediction of the CNN (dark grey = axons, light grey = axonal swellings, white = axonal fragments), backpropagation alters the connections among the nodes by readjusting the weights. Scale bar: 100 μm. AxD: Axonal degeneration; CNN: convolutional neural network. Unpublished data.

Box 1 Comparison of different deep learning-based approaches to quantify features of AxD:

Deep learning-based approach	TrailMap (Friedmann et al., 2020)	CMN (Schubert et al., 2019)	AxonDeepSeg (Zaimi et al., 2018)	DeepBouton (Cheng et al., 2019)	EntireAxon (Menon et al., 2020; Palumbo et al., 2021)
Specimen	Whole tissue *ex vivo*	Tissue slices *ex vivo*	Tissue slices *ex vivo*	Whole tissue *ex vivo*	Spatially isolated axons in microfluidic device *in vitro*
Microscopy	Light sheet microscopy	Electron microscopy	Electron microscopy	High-resolution stage-scanning confocal microscopy	Phase-contrast and fluorescence microscopy, time-lapse imaging
Networks	3D CNN based on u-net	Cellular morphology neural networks based on multiview CNN	CNN based on u-net	CNN based on u-net with ResNet-50	Ensemble of CNNs, based on u-net with ResNet-50, recurrent neural network
Learning strategy	Supervised	Supervised and unsupervised	Supervised	Supervised	Supervised
Recognized structures	Axons	Axons, dendrites, and somata	Axons and myelin	Axonal swellings	Axons, axonal swellings, and axonal fragments
Outcome parameters	Axon density	Reconstruction of volume and localization of axons, dendrites, and somata	Volume, diameter, and density of axons and myelin, G-ratio	Number of axonal swellings	Area of axons, axonal swellings, and axonal fragments, degeneration patterns

Alex Palumbo, Marietta Zille*
Department of Neurobiology, Harvard Medical School; Department of Cancer Biology, Dana-Farber Cancer Institute, Boston, MA, USA (Palumbo A)
Department of Pharmaceutical Sciences, Division of Pharmacology and Toxicology, University of Vienna, Vienna, Austria (Zille M)
*Correspondence to: Marietta Zille, PhD, marietta.zille@univie.ac.at.
https://orcid.org/0000-0002-0609-8956 (Marietta Zille)

References

Arrázola MS, Saquel C, Catalán RJ, Barrientos SA, Hernandez DE, Martínez NW, Catenaccio A, Court FA (2019) Axonal degeneration is mediated by necroptosis activation. J Neurosci 39:3832-3844.

Canty AJ, Jackson JS, Huang L, Trabalza A, Bass C, Little G, Tortora M, Khan S, De Paola V (2020) In vivo imaging of injured cortical axons reveals a rapid onset form of Wallerian degeneration. BMC Biol 18:170.

Cheng S, Wang X, Liu Y, Su L, Quan T, Li N, Yin F, Xiong F, Liu X, Luo Q, Gong H, Zeng S (2019) DeepBouton: automated identification of single-neuron axonal boutons at the brain-wide scale. Front Neuroinform 13:25.

Friedmann D, Pun A, Adams EL, Lui JH, Kebschull JM, Grutzner SM, Castagnola C, Tessier-Lavigne M, Luo L (2020) Mapping mesoscale axonal projections in the mouse brain using a 3D convolutional network. Proc Natl Acad Sci U S A 117:11068-11075.

Gerdts J, Brace EJ, Sasaki Y, DiAntonio A, Milbrandt J (2015) SARM1 activation triggers axon degeneration locally via NAD⁺ destruction. Science 348:453-457.

Grüning P, Palumbo A, Zille M, Barth E, Madany Mamlouk AA (2020) A task-dependent active learning method for axon segmentation with CNNs. Proc AUTOMED 1:25.

Kerschensteiner M, Schwab ME, Lichtman JW, Misgeld T (2005) In vivo imaging of axonal degeneration and regeneration in the injured spinal cord. Nat Med 11:572-577.

Knöferle J, Koch JC, Ostendorf T, Michel U, Planchamp V, Vutova P, Tonges L, Stadelmann C, Bruck W, Bahr M, Lingor P (2010) Mechanisms of acute axonal degeneration in the optic nerve in vivo. Proc Natl Acad Sci U S A 107:6064-6069.

Menon NK, Palumbo A, Grüning P, Landt SK, Heckmann L, Bartram L, Madany Mamlouk A, Zille M (2020) Segmentation of fluorescently labelled axons in a model of brain hemorrhage-induced axonal degeneration using convolutional neural networks. In: Student Conference proceedings 2020: 9th Conference on Medical Engineering Science, 5th Conference on Medical Informatics, 3rd Conference on Biomedical Engineering, 2nd Conference on Auditory Technology. (Buzug TM, ed), pp229-233. Lübeck: Infinite Science Publishing.

Palumbo A, Grüning P, Landt SK, Heckmann LE, Bartram L, Pabst A, Flory C, Ikhsan M, Pietsch S, Schulz R, Kren C, Koop N, Boltze J, Madany Mamlouk A, Zille M (2021) Deep learning to decipher the progression and morphology of axonal degeneration. Cells 10:2539.

Sasaki Y, Vohra BPS, Lund FE, Milbrandt J (2009) Nicotinamide mononucleotide adenylyl transferase-mediated axonal protection requires enzymatic activity but not increased levels of neuronal nicotinamide adenine dinucleotide. J Neurosci 29:5525-5535.

Schubert PJ, Dorkenwald S, Januszewski M, Jain V, Kornfeld J (2019) Learning cellular morphology with neural networks. Nat Commun 10:2736.

Yang GR, Wang XJ (2020) Artificial neural networks for neuroscientists: a primer. Neuron 107:1048-1070.

Yong HYF, Rawji KS, Ghorbani S, Xue M, Yong VW (2019) The benefits of neuroinflammation for the repair of the injured central nervous system. Cell Mol Immunol 16:540-546.

Zaimi A, Wabartha M, Herman V, Antonsanti P-L, Perone CS, Cohen-Adad J (2018) AxonDeepSeg: automatic axon and myelin segmentation from microscopy data using convolutional neural networks. Sci Rep 8:3816.

C-Editors: Zhao M, Liu WJ, Wang Lu; T-Editor: Jia Y